Formation of regular arrays of silicon microspikes by femtosecond laser irradiation through a mask

M. Y. Shen,[a] C. H. Crouch, J. E. Carey, R. Younkin, and E. Mazur
Department of Physics and Division of Engineering and Applied Sciences, Harvard University, Cambridge, Massachusetts 02138

M. Sheehy and C. M. Friend
Department of Chemistry, Harvard University, Cambridge, Massachusetts 02138

(Received 3 October 2002; accepted 22 January 2003)

We report fabrication of regular arrays of silicon microspikes by femtosecond laser irradiation of a silicon wafer covered with a periodic mask. Without a mask, microspikes form, but they are less ordered. We believe that the mask imposes order by diffracting the laser beam and providing boundary conditions for capillary waves in the laser-melted silicon. © *2003 American Institute of Physics.* [DOI: 10.1063/1.1561162]

A variety of micrometer-scale surface patterns have been observed on silicon surfaces after pulsed laser irradiation.[1–6] When irradiated by nanosecond laser pulses at a fluence close to the melting threshold, silicon surfaces develop ripples with submicrometer periodicity (often called laser-induced periodic surface structures, or LIPSS).[1,7] By irradiating surfaces with femtosecond laser pulses above the ablation threshold in SF_6, we previously created silicon surfaces covered with a semi-ordered pattern of sharp conical microspikes.[3,4] Others have also reported laser-induced formation of larger conical microstructures using high-intensity nanosecond pulses.[2,5,6]

While the mechanism responsible for LIPSS formation is now well understood, the mechanism of microspike formation is not. To better understand this mechanism, we imposed boundary conditions on the excited silicon surface and the incident laser light by irradiating the silicon surface through a periodic mask. The resulting microspikes are arranged in regular arrays with the same symmetry as the mask apertures. The arrangement and separation of the microspikes indicate that capillary waves in the molten silicon may play a role in microspike formation; ordering may arise from confinement of the region of laser-melted silicon at the surface combined with diffraction of the laser light.

We masked silicon chips [float zone Si(111)] by affixing 2-μm-thick copper transmission electron microscope (TEM) grids to the sample surface with conductive carbon tape. The carbon tape causes a gap between the silicon surface and the TEM grid, varying from a few micrometers to tens of micrometers. We used square grids of width 10, 20, 30, 40, 50, and 200 μm, and hexagonal grids of width 30 μm. The sample is mounted normal to the laser beam on a three-axis translation stage in a vacuum chamber with a base pressure of less than 10^{-2} Pa. During sample irradiation, the chamber is backfilled with 6.7×10^4 Pa SF_6. The laser pulses (800 nm, 100 fs, 0.3 mJ) are focused to a beam waist of 200 μm at the sample surface; the spatial profile of the beam is Gaussian, and the fluence per pulse at the sample surface is 6 kJ/m^2, which is well above the thresholds for both ablation and plasma formation. The sample is translated at 200 μm/s in the plane perpendicular to the laser beam, and a fast shutter is used to vary the repetition rate of the laser pulse train between 5 and 50 Hz, thereby controlling the average number of laser pulses per unit area.[8] After irradiation, the masks are removed and the resulting structures imaged with a scanning electron microscope.

Figures 1(a) and 1(b) are electron micrographs of the surfaces obtained using a mask with 30-μm hexagonal openings; Figs. 1(c) and 1(d) show surfaces obtained using a mask with 20-μm square openings. The microspikes are arranged in regular arrays with the same symmetry as the mask. The gray bars above Figs. 1(a) and 1(b) show the spatial intensity profile of the laser beam; the density of the microspikes depends on the laser fluence, with a higher density of microspikes forming where the fluence is less. Along a constant-fluence line perpendicular to the laser intensity profile, the density and arrangement of microspikes is nearly uniform. Using a mask with 10-μm or 30-μm square openings also produces ordered microspikes of the same number density as the 20-μm square openings; using a mask with larger openings produces ordered microspikes at the edges, but the microspikes in the center of the opening are quasi-ordered, like the microspikes produced without a mask.

Figures 2(a)–2(e) show the development of the microspikes as the number of laser pulses increases, using a mask with square openings, and with the laser polarization parallel to the vertical axis of the mask. After five laser pulses, periodic ripples form with the same wavelength as the laser light (800 nm), oriented perpendicular to the polarization of the laser light. Between 10 and 50 pulses, a coarser periodic structure appears on top of the ripples, consisting of ridges parallel to the polarization of the light and perpendicular to the underlying ripple structure. In the absence of a mask, periodic ripples also form perpendicular to the laser polarization, but the subsequent coarser structure lacks the order of the structures shown in Fig. 2.[9] Between 100 and 200 pulses, the underlying ripples vanish, and the coarsened structure evolves into an ordered array of microspikes. If the laser polarization is rotated 45° relative to the sides of the

[a]On leave from Tohoku University, Sendai, Japan; electronic mail: mshen@deas.harvard.edu

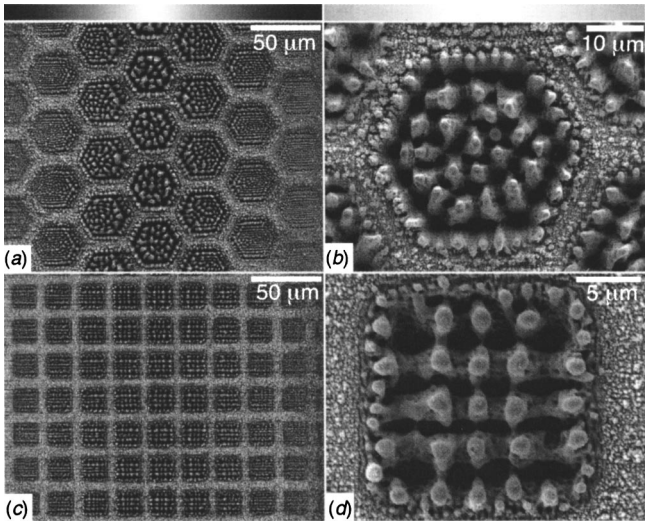

FIG. 1. Scanning electron micrographs of ordered silicon spikes formed by masking the irradiated sample with (a), (b) a 30-μm hexagonal grid and (c), (d) a 20-μm square grid. The nearly Gaussian spatial intensity profile of the laser pulse is shown at the top in grayscale (white corresponds to maximum intensity).

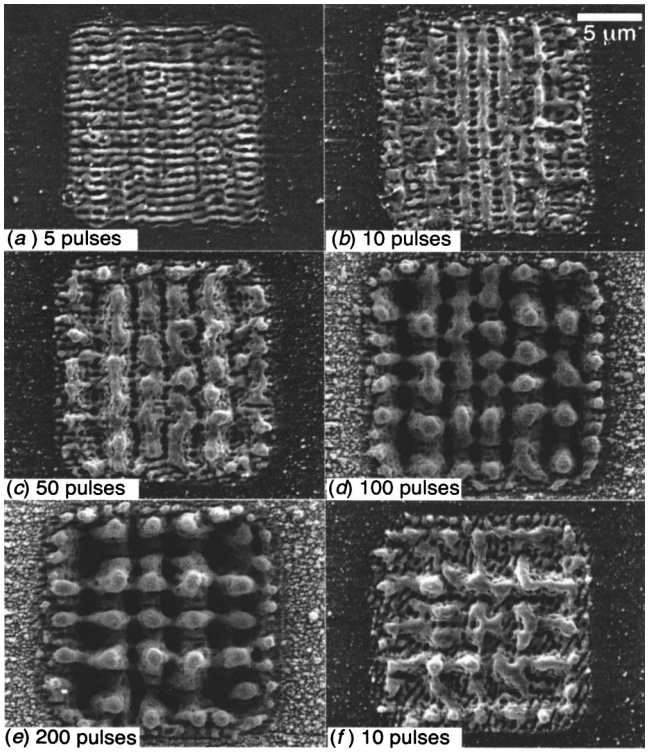

FIG. 2. Scanning electron micrographs of (a)–(e) silicon spikes formed with a square grid after increasing number of laser pulses. The direction of the electric field is vertical in (a)–(e). (f) Spikes formed with the grid rotated 45° relative to the grids in (a)–(e).

mask openings, as in Fig. 2(f), the coarsened structure that exists after 10 pulses no longer consists of ridges parallel to the polarization, as in Fig. 2(b). Instead, the coarsened structure is fragmented into smaller structures, and those structures fall roughly on a square array with axes parallel to the sides of the mask openings.

We identify three stages in the process of spike formation from the images presented in Fig. 2. First, ripples form on the silicon surface, then a coarsened layer forms on top of the ripples, and finally the coarsened layer fragments into beads which subsequently are etched into microspikes. In the remainder of this letter, we will discuss possible mechanisms for this process.

Periodic ripple formation upon laser irradiation of solids with nanosecond pulses below the ablation threshold has been previously reported, and was attributed to periodic melting of strips on the surface (at low fluence) or capillary wave formation in a uniformly melted area (at high fluence).[7] Under the conditions we use, with each laser pulse, a plasma forms; after the plasma expands, a molten silicon layer is left behind on the surface, which solidifies before the next laser pulse arrives. The ripples we observe [Fig. 2(a)] have the same wavelength as the laser wavelength; we therefore expect that as in the nanosecond case, ripple formation is due to capillary waves excited in the molten silicon by interference between the incident and scattered laser light.[7]

Formation of the coarsened layer and subsequent fragmentation into microspikes could either involve plasma oscillations[10] or capillary waves in the molten silicon.[6] In addition, Fresnel diffraction of the incident light from the edges of the mask openings[11] should produce a modulated temperature profile in the plasma or the liquid; temperature variations may play a role in exciting or sustaining the oscillations.

Let us first consider the possibility of a plasma oscillation induced by the trailing edge of the light pulse. By analyzing the radiation backscattered from a laser-produced plasma, Jannitti and coworkers[10] observed a resonant interaction between the plasma and laser pulse light when the plasma frequency equals the laser light frequency. This resonance occurs because the electron density of the plasma increases with increasing laser fluence; the corresponding plasma frequency can therefore increase until the plasma frequency is resonant with the laser light frequency, and the electromagnetic field couples directly to the plasma oscillation. However, we find that increasing the fluence increases both the typical separation of the microspikes [Figs. 1(a) and 1(c)] and the wavelength of the coarsened layer. If the microspike separation was determined by the plasmon wavelength, increasing the plasma density, and therefore the plasma frequency, should instead decrease the typical separation of the microspikes and the wavelength of the coarsened layer. Therefore plasma oscillations cannot be responsible for the arrangement of the microspikes.

Let us next consider capillary waves in the molten silicon as a mechanism for forming the coarsened layer. Diffraction of the laser light from the mask apertures causes inhomogeneous energy deposition into the substrate; as a result, the temperature in the molten surface layer is periodically modulated. The surface tension of the molten silicon decreases with increasing temperature, so the hot liquid flows toward cooler regions, deforming the surface. Relaxation of the deformation as the molten silicon cools can then excite capillary waves in the molten liquid; these capillary waves are most likely the instability that drives both the formation of the coarsened layer and its subsequent breakup.

We can estimate the characteristic length scale of the coarsened layer from the dispersion relation for capillary waves in a shallow liquid layer:[6,12]

$$\lambda = \left[\frac{\sigma d}{\rho}\right]^{1/4} (2\pi\tau)^{1/2}, \quad (1)$$

where λ and τ are the wavelength and period of the capillary waves, respectively and σ, d, and ρ are the surface tension coefficient, depth, and mass density of the liquid layer, respectively. Note that the capillary wave period cannot exceed the lifetime of the liquid layer τ_{liq}, and therefore the average spike separation λ_{spike} cannot exceed the wavelength corresponding to τ_{liq}. We estimate τ_{liq} to be between 75 ns (a value measured by others with somewhat lower fluence at a shorter wavelength[13]) and 600 ns (calculated from a simple model that ignores the effect of ablation[14]). The penetration depth α^{-1} of 800-nm light into silicon is roughly 10 μm,[15] and others have determined that the liquid layer formed at lower fluence and shorter wavelength is roughly 100 nm deep;[13] we therefore expect the liquid layer depth d to lie between these two limits. Using these ranges of values for τ_{liq} and d and literature values for σ and ρ[16,17] in Eq. (1), we estimate the longest allowed wavelength to be between 2 and 20 μm. The observed λ_{spike} of 5 μm (Figs. 1 and 2) falls nicely in this range of values.

The observed increase of the average spike separation with increasing fluence is also consistent with capillary wave-driven formation. Increasing the fluence deposits more energy in the silicon substrate, melting more silicon and therefore increasing the liquid layer depth and lifetime. The dispersion relation given above indicates that increased depth and lifetime should correspond to a longer wavelength.

When the melted silicon layer is confined rather than infinite in extent, the size of the melted area constrains the allowed capillary wavelengths, and standing waves form. In a melted square with side a, allowed standing wave vectors are given by $k = \pi m/a$ $(m = 1,2,3,...)$. As we observe only a single wavelength in all the squares irradiated with a given fluence, some additional mechanism must be at work to select a particular wavelength. Fresnel diffraction from the edges of the mask opening cannot on its own determine the arrangement of the microspikes, as the spatial period of a diffraction pattern is independent of laser fluence and therefore cannot produce a fluence-dependent arrangement of microspikes. However, the diffraction pattern may help select a particular capillary wavelength. We calculated the power spectrum of the diffracted light intensity on the silicon surface, and find that the peak amplitude decreases with increasing m.[18] Consequently, diffraction should promote formation of the longest wavelength capillary wave that can exist given the lifetime of the melted layer. When the grid opening is larger than 30 μm, the diffraction pattern is only significant near the edges of the openings, and so ordering only occurs there.

The dependence of the structures on laser polarization is also consistent with a formation mechanism involving both capillary wave excitation and Fresnel diffraction. Because the mask is conducting, the tangential electrical field at the edges of the mask must be zero. When the polarization is parallel to one pair of sides of the square aperture, as shown in Fig. 2(b) the intensity of the electric field is zero along the parallel sides and nonzero along the perpendicular sides, which may promote formation of wavefronts parallel to one pair of parallel sides. When the polarization can be decomposed into roughly equal components along both pairs of sides, as in Fig. 2(f), standing waves form parallel to both pairs of sides.

In conclusion, we form micrometer-scale regions containing ordered arrays of silicon microspikes by femtosecond laser-assisted etching of silicon with periodic masks. We attribute this ordering to the selection of particular capillary waves in the molten silicon by Fresnel diffraction of light from the mask aperture. These ordered arrays of microspikes could find application as pixels of microspikes for field-emission devices and detectors.

This work was supported by the Harvard MRSEC (NSF/DMR-98-09363) and the Department of Energy. The authors thank J. Ashcom for experimental assistance, and Profs. H. Stone and M. Brenner for helpful discussions.

[1] P. M. Fauchet and A. E. Siegman, Appl. Phys. Lett. **40**, 824 (1982).
[2] J. E. Rothenberg and R. Kelly, Nucl. Instrum. Methods Phys. Res. B **1**, 291 (1984).
[3] T.-H. Her, R. J. Finlay, C. Wu, S. Deliwala, and E. Mazur, Appl. Phys. Lett. **73**, 1673 (1998).
[4] T.-H. Her, R. J. Finlay, C. Wu, and E. Mazur, Appl. Phys. A: Mater. Sci. Process. **70**, 383 (2000).
[5] A. J. Pedraza, J. D. Fowlkes, and D. H. Lowndes, Appl. Phys. Lett. **74**, 2322 (1999).
[6] S. I. Dolgaev, S. V. Lavrishev, A. A. Lyalin, A. V. Simakin, V. V. Voronov, and G. A. Shafeev, Appl. Phys. A: Mater. Sci. Process. **73**, 177 (2001).
[7] J. E. Sipe, J. F. Young, J. S. Preston, and H. M. van Driel, Phys. Rev. B **27**, 1141 (1983).
[8] We find that the spike formation is almost independent of the laser pulse train frequency when the laser repetition rate is slower than 100 Hz and the translation velocity is 200 μm/s. Thus we simply vary the repetition rate (determined by the shutter) to control the average number of light pulses incident on the silicon surface.
[9] C. H. Crouch, M. Y. Shen, J. E. Carey, and E. Mazur (unpublished).
[10] E. Jannitti, A. M. Malvezzi, and G. Tondello, J. Appl. Phys. **46**, 3096 (1975).
[11] M. Born and E. Wolf, *Principles of Optics*, 7th ed. (Cambridge University Press, Cambridge, UK, 1999), p. 481.
[12] L. D. Landau and E. M. Lifshitz, *Hydrodynamics* (Nauka, Moscow, 1988).
[13] K. Sokolowski-Tinten, J. Bialkowski, A. Cavalleri, D. von der Linde, A. Oparin, J. Meyer-ter-Vehn, and S. I. Anisimov, Phys. Rev. Lett. **81**, 224 (1998).
[14] $\tau_{liq} \sim (2D)^{-1}\alpha^{-2}$, where D is the thermal diffusivity and α^{-1} the penetration depth; from N. Bloembergen, AIP Conf. Proc. **50**, 1 (1979).
[15] $\alpha^{-1} = \lambda/(4\pi\kappa)$, with $\lambda = 800$ nm and $\kappa = 0.007$; κ is obtained from Palik, *Handbook of Optical Constants of Solids* (Academic, Chestnut Hill, MA, 1998), Vol. 1.
[16] *CRC Handbook of Chemistry and Physics*, 66th ed. (CRC Press, Boca Raton, FL, 1985–1986) p. F-25.
[17] C. Kittel, *Introduction to Solid State Physics*, 5th ed. (Wiley, New York, 1976), p. 32.
[18] The power spectrum shows that the component with wave vector k depends on the gap between the silicon surface and the TEM grid. The amplitude decreases as m increases, except that the component with $m = 2$ has near-zero amplitude for the range of gap values corresponding to our experiment. As we observe structures only with $m \geqslant 3$, we expect that $m = 1$ corresponds to a lifetime too great to be observed.